IEEE Access
Multidisciplinary | Rapid Review | Open Access Journal

Received December 4, 2019, accepted January 4, 2020, date of publication January 10, 2020, date of current version January 21, 2020.

Digital Object Identifier 10.1109/ACCESS.2020.2965744

A Novel Fault Diagnosis Approach for Rolling Bearing Based on High-Order Synchrosqueezing Transform and Detrended Fluctuation Analysis

WEI LIU[1,2], WEI CHEN[3,4], AND ZHIHUA ZHANG[1,2]

[1]College of Mechanical and Electrical Engineering, Beijing University of Chemical Technology, Beijing 100029, China
[2]Beijing Key Laboratory of Health Monitoring Control and Fault Self-Recovery for High-End Machinery, Beijing University of Chemical Technology, Beijing 100029, China
[3]Key Laboratory of Exploration Technology for Oil and Gas Resources of Ministry of Education, Yangtze University, Wuhan 430100, China
[4]Hubei Cooperative Innovation Center of Unconventional Oil and Gas, Wuhan 430100, China

Corresponding author: Wei Chen (chenwei_yangtze@126.com)

This work was supported by the Fundamental Research Funds for the Central Universities of China under Grant ZY1916.

ABSTRACT Time-frequency analysis always plays an important role in machine health monitoring owing to its advantage in extracting the fault information contained in non-stationary signal. In this paper, we present a novel technique to detect and diagnose the rolling bearing faults based on high-order synchrosqueezing transform (FSSTH) and detrended fluctuation analysis (DFA). With this method, the high-order synchrosqueezing transform is first utilized to decompose the vibration signal into an ensemble of oscillatory components termed as intrinsic mode functions (IMFs). Meanwhile, an empirical equation, which is based on the DFA, is introduced to adaptively determine the number of IMFs from FSSTH. Then, a time-frequency representation originated from the decomposed modes or corresponding envelopes is exhibited in order to identify the fault characteristic frequencies related to rolling bearing. Experiments are carried out using both simulated signal and real ones from Case Western Reserve University. Results show that the proposed method is more effective for the detection of fault characteristic frequencies compared with the traditional synchrosqueezing transform (SST) based fault diagnosis algorithm, which renders this technique is promising for machine fault diagnosis.

INDEX TERMS Fault diagnosis, rolling bearing, time-frequency analysis, high-order synchrosqueezing transform, detrended fluctuation analysis.

I. INTRODUCTION

Rolling bearing is widely used in various industrial machines and is considered one of the most stressed parts in rotating machinery. In fact, bearing is prone to failure due to long-term impact and overload [1]–[4]. Once a fault occurs in rolling bearing, it will lead to expensive production shutdowns in manufacturing industry [5]. Therefore, machine condition monitoring is of great importance to ensure the safe and efficient operation of equipment.

Time-frequency analysis method has been widely applied in machine fault diagnosis because it is capable of providing the localization information related with the non-stationary signal both in time and frequency domains [6], [7]. Commonly used approaches are short-time Fourier transform (STFT) [8], [9] and wavelet transform (WT) [10], [11]. Unfortunately, both have the limitation, namely that one cannot accomplish the high resolutions in time and frequency domains simultaneously [12]. Aiming at this problem, great efforts have been made. In 1995, Auger and Flandrin [13] proposed a reassignment method (RM) on the time-frequency plane, which can improve the time-frequency localization to some extent [14]. However, RM is not invertible, which means that it is impossible for recovering the original signal. S-transform, proposed by Stockwell *et al.* [15], combines the elements of STFT and WT. A signal from the time domain can be decomposed into the time-frequency plane directly via the S-transform [16]. Wigner-Ville distribution (WVD) [17], [18] obtains a higher time-frequency resolution, but it suffers from the cross-term interferences as a result of its quadratic nature, which hinders the readability in the multicomponent case, thus is not suitable for many real

The associate editor coordinating the review of this manuscript and approving it for publication was Jun Shen.

applications. Matching pursuit (MP) [19], [20] provides an alternative for time-frequency analysis, which implements the signal decomposition in the over-complete dictionaries. It achieves the higher time-frequency resolution, but at the expense of an increased computational cost. Empirical mode decomposition (EMD) [21], [22] and its extensions ensemble EMD (EEMD) [23], [24] and complete EEMD (CEEMD) [25], [26] belong to the adaptive non-parametric algorithms. Despite their considerable success in many fields, there is still a lack of solid theory foundation and a high computational complexity. In 2011, Daubechies and Wu [27] introduced a wavelet-based time-frequency representation by means of frequency reassignment, called sychrosqueezing transform (SST) that initially originated from the field of audio signal analysis [28], it aims to improve the time-scale representation resulted from continuous wavelet transform (CWT) [29]. Subsequently, Thakur and Wu [30] developed an extension of SST to the time-frequency representation given by STFT, termed as STFT-based SST (FSST). Although the FSST obtains the enhanced time-frequency resolution, it encounters some difficulties when coping with the signals with ''fast varying'' instantaneous frequency because of the requirement of weak frequency modulation hypothesis for the modes comprising the signal. Since then, a lot of attempts have being made to deal with this issue. In 2017, Pham and Meignen [31] proposed a new adaptive signal analysis algorithm that is known as high-order synchrosqueezing transform (FSSTH). It is a new generalization of the STFT-based synchrosqueezing transform by computing more accurate estimates of the instantaneous frequencies using higher order approximations both for the amplitude and phase, which results in perfect concentration and reconstruction for a wider variety of signals. Currently, FSSTH has successfully been applied to the analysis of a transient gravitational-wave signal [31], seismic time-frequency analysis [12] and machine fault diagnosis [32], [33]. However, the determination of the number of IMFs from FSSTH does not been investigated, which is key for non-stationary signal characterization and effective feature extraction.

In this paper, we propose a metric based on detrended fluctuation analysis (DFA) to determine the number of IMFs from FSSTH, and present a new method for the fault detection of rolling bearing, which makes full use of the advantage of FSSTH in extracting instantaneous frequencies with higher precision. Firstly, the input signal is decomposed into a series of oscillatory components adaptively by FSSTH; meanwhile, the DFA is employed as a robust metric to determine the optimal number of IMFs. Then, a time-frequency representation that relates to the decomposed IMFs or corresponding envelopes is obtained in order to identify the fault characteristic frequencies associated with rolling bearing. Both simulated signal and experimental vibration signals from Case Western Reserve University have verified the performance of the proposed method on fault diagnosis for rolling bearing.

The rest of the paper is organized as follows. In section II, we depict the fundamental theory of high-order synchrosqueezing transform, detrended fluctuation analysis, and the proposed fault diagnosis algorithm for rolling bearing. Section III illustrates the simulation test of the method by numerical signal analysis. In section IV, the effectiveness and robustness of the proposed approach in the rolling bearing fault diagnosis is further verified using two experimental signals. Finally, conclusions are drawn in Section V.

II. THE PROPOSED METHOD

A. HIGH-ORDER SYNCHROSQUEEZING TRANSFORM

The high-order synchrosqueezing transform is a new extension of the conventional STFT-based SST (FSST) that was firstly proposed by Thakur and Wu [30], which achieves more accurate estimates of the instantaneous frequencies by using higher order approximations both for the amplitude and phase [31].

An AM-FM signal is described as:

$$f(t) = A(t)\, e^{i2\pi\phi(t)}. \tag{1}$$

where $A(t)$ and $\phi(t)$ denote the amplitude and phase functions, respectively.

The STFT of signal f can be defined as:

$$V_f^g(t,\eta) = \int f(\tau) g^*(\tau - t)\, e^{-i2\pi\eta(\tau-t)} d\tau. \tag{2}$$

where g is the window function and g^* is the complex conjugate of g.

The traditional STFT-based SST (FSST) is defined as follows:

$$T_f^{g,\gamma}(t,\omega) = \frac{1}{g^*(0)} \int_{\left\{\eta,\left|V_f^g(t,\eta)\right|>\gamma\right\}} V_f^g(t,\eta)\, \delta\left(\omega - \omega_f(t,\eta)\right) d\eta, \tag{3}$$

where γ is the threshold and δ is the Dirac distribution. $\omega_f(t,\eta)$ denotes the instantaneous frequency estimate at time t and frequency η and is estimated as:

$$\omega_f(t,\eta) = R\left\{\frac{\partial_t V_f^g(t,\eta)}{i2\pi V_f^g(t,\eta)}\right\}. \tag{4}$$

where $R\{Z\}$ represents the real part of complex number Z, and ∂_t is the partial derivative with respect to t.

The high-order SST computes the instantaneous frequency by using the high order Taylor expansions of the amplitude and phase, namely, the Taylor expansions of signal f in equation (1) for τ close to t can be expressed as:

$$f(\tau) = \exp\left(\sum_{k=0}^{N} \frac{\left[\log(A)\right]^{(k)}(t) + i2\pi\phi^{(k)}(t)}{k!} (\tau - t)^k\right). \tag{5}$$

where $Z^{(k)}(t)$ is the kth derivative of Z at time t.

Therefore, equation (2) can be rewritten as:

$$V_f^g(t,\eta) = \int f(\tau+t)g^*(\tau)\,e^{-i2\pi\eta\tau}d\tau = \int \exp\left(\sum_{k=0}^{N}\frac{[\log(A)]^{(k)}(t)+i2\pi\phi^{(k)}(t)}{k!}\tau^k\right) \times g^*(\tau)\,e^{-i2\pi\eta\tau}d\tau. \quad (6)$$

The local instantaneous frequency estimate, $\omega_f(t,\eta)$, can be obtained via equation (4).

$$\omega_f(t,\eta) = \frac{[\log(A)]'(t)}{i2\pi} + \phi'(t) + \sum_{k=2}^{N}\frac{[\log(A)]^{(k)}(t)+i2\pi\phi^{(k)}(t)}{i2\pi\,(k-1)!}\frac{V_f^{t^{k-1}g}(t,\eta)}{V_f^g(t,\eta)}. \quad (7)$$

Introduce the frequency modulation operator $q_{\eta,f}^{[k,N]}$:

$$q_{\eta,f}^{[k,N]} = \frac{[\log(A)]^{(k)}(t)+i2\pi\phi^{(k)}(t)}{i2\pi\,(k-1)!}, \quad (8)$$

The Nth-order local complex instantaneous frequency, $\omega_{\eta,f}^{[N]}$ at time t and frequency η, can be represented by:

$$\omega_{\eta,f}^{[N]}(t,\eta) = \begin{cases} \omega_f(t,\eta) + \sum_{k=2}^{N} q_{\eta,f}^{[k,N]}(\eta,t)\left(-x_{k,1}(t,\eta)\right), \\ V_f^g(t,\eta)\neq 0,\ \partial_\eta x_{j,j-1}(t,\eta)\neq 0\ (j\geq 2). \\ \omega_f(t,\eta), \\ otherwise. \end{cases} \quad (9)$$

As a result, the high-order FSST is defined by using $\omega_{\eta,f}^{[N]}(t,\eta)$ instead of $\omega_f(t,\eta)$ in equation (3):

$$T_{N,f}^{g,\gamma}(t,\omega) = \frac{1}{g^*(0)}\int_{\left\{\eta,\left|V_f^g(t,\eta)\right|>\gamma\right\}} V_f^g(t,\eta)\,\delta\left(\omega-\omega_{\eta,f}^{[N]}(t,\eta)\right)d\eta. \quad (10)$$

Finally, the mode can be approximately reconstructed by:

$$f(t) \approx \int_{\{\omega,|\omega-\varphi(t)|<d\}} T_{N,f}^{g,\gamma}(t,\omega)d\omega. \quad (11)$$

where d denotes the compensation factor and $\varphi(t)$ is an estimate for $\phi'(t)$.

B. DETRENDED FLUCTUATION ANALYSIS

Detrended fluctuation analysis (DFA) proposed by Peng *et al.* [34] is a successful method to measure long-range dependency for the non-stationary time series.

The first step of the algorithm is that the average is removed from the time series:

$$y(k) = \sum_{i=1}^{k}[x(i)-\bar{x}], \quad 1\leq k\leq N, \quad (12)$$

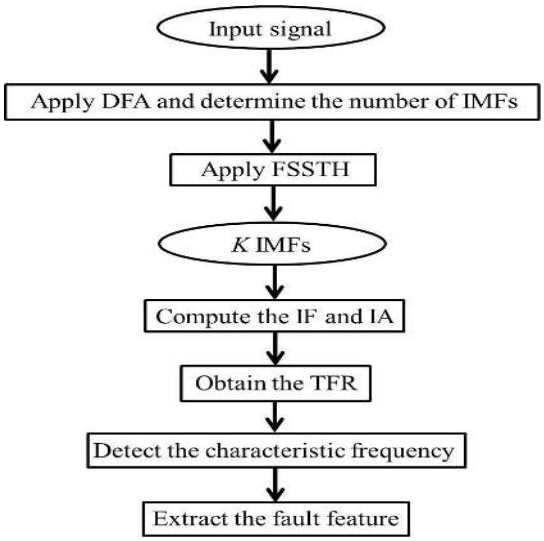

FIGURE 1. Flowchart of the proposed method.

where $\bar{x}$ is the average of the time series within the range $[1, N]$, and N is the number of samples.

Then, the average root mean square (RMS) fluctuation $F(n)$ is obtained by subtracting $y_n(k)$ from the time series $y(k)$ as defined below:

$$F(n) = \sqrt{\frac{1}{N}\sum_{k=1}^{N}[y(k)-y_n(k)]^2}, \quad (13)$$

where $y_n(k)$ is the estimated local trend in the box size n.

If the time series is long-range power-law corrected, the fluctuation increases via a power law:

$$F(n) \propto n^{\alpha}. \quad (14)$$

The scaling exponent α is defined as the slope of the plot of $\log[F(n)]/\log(n)$, which is estimated in log-log scale. It provides a clear and quantitative score caused by the temporal correlations existing in the time series [35]. Generally speaking, the scaling exponent yields $\alpha = 0.5$ for completely uncorrelated data. When $0 < \alpha < 0.5$, the signal is anti-correlated. When α is in the range between 0.5 and 1.0, temporal correlations exist [36]. DFA has become a widely used technique for determination of scaling properties and detection of long-range correlations in non-stationary time series owing to its reliable ability of detrending the time series [37]. In the paper, we utilize the DFA to determine the number of IMFs from FSSTH.

C. PROCEDURE OF THE PROPOSED METHOD FOR ROLLING BEARING FAULT DIAGNOSIS

The proposed method is mainly composed of FSSTH and DFA, the overall structure of this method is illustrated in Figure 1. The detailed implementation procedure for fault diagnosis is summarized as follows:

1) Collect the vibration signal.

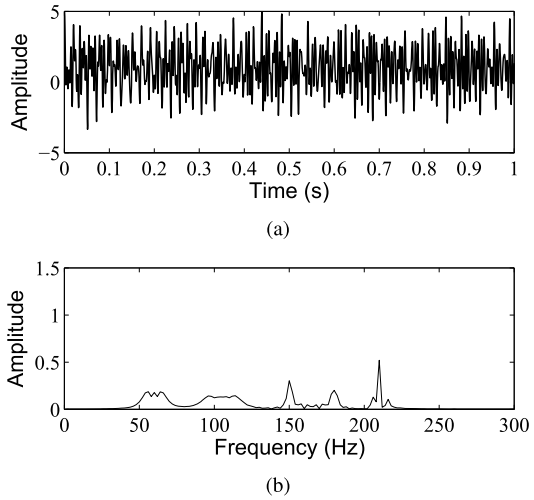

FIGURE 2. Time-domain waveform (a) and Fourier spectrum (b) of the simulated signal.

2) Use the FSSTH to decompose the input signal and obtain an ensemble of oscillatory components (IMFs).

3) Estimate the scaling exponent regarding each IMF via the DFA to determine the number of IMFs from FSSTH.

4) Compute the instantaneous frequency (IF) and instantaneous amplitude (IA) of each IMF or corresponding envelope.

5) Obtain the time-frequency representation (TFR).

6) Detect the characteristic frequency and extract the fault feature.

III. SIMULATION TEST

To test the performance of the proposed method, we consider a simulated signal $s(t)$ generated by equation (15), which consists in two FM components $s_1(t)$, two frequency-varying cosine components $s_2(t)$, and an AM cosine component $s_3(t)$. The sampling frequency is 2048Hz. The waveform and spectrum of $s(t)$ are shown in Figures 2(a) and (b), respectively. It can be clearly seen that the Fourier spectrum nearly exhibits each component that comprises the simulated signal.

$$\begin{aligned} s_1(t) &= \cos\left(2\pi 50t + 2\pi 20t^2\right) + \cos\left(2\pi 90t + 2\pi 30t^2\right), \\ s_2(t) &= \begin{cases} \cos(2\pi 150t), & t < 0.3 \\ \cos(2\pi 180t), & t \geq 0.3 \end{cases}, \\ s_3(t) &= [1 + 0.5\sin(2\pi 5t)]\cos(2\pi 210t), \\ s(t) &= s_1(t) + s_2(t) + s_3(t). \end{aligned} \tag{15}$$

Now, the FSSTH is employed to decompose the simulated signal $s(t)$. To make the FSSTH adaptive, we need to determine the optimal number of IMFs (K) in a data-driven way. In the paper, we utilize an empirical equation for the determination of K [36]:

$$K = \min\left\{n \in Z^+ | n \geq 2\alpha \lg(N)\right\}. \tag{16}$$

where α is the scaling exponent from DFA of the input signal.

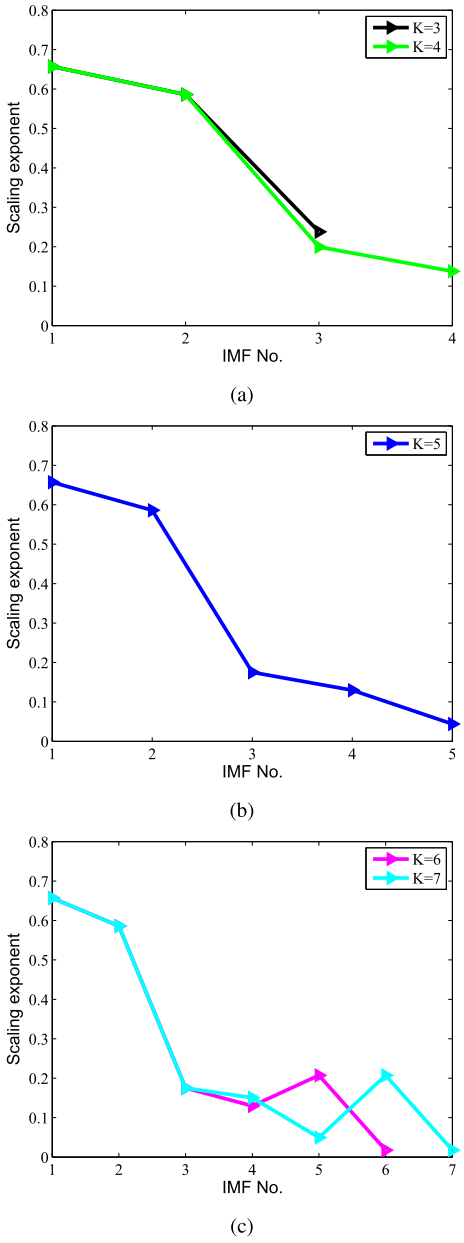

FIGURE 3. Scaling exponents with different IMFs from FSSTH, (a) $K = 3, 4$; (b) $K = 5$; (c) $K = 6, 7$.

Figure 3 shows the variation of scaling exponents with the number of IMFs from FSSTH, and the values are listed in Table 1. The first IMFs with larger scaling exponent are mostly comprised of high relevant components while the last IMFs with lower scaling exponent mainly carry the components with low correlation. As shown in Figure 3, if the K is lower, for example 3 and 4, the IMFs are highly relevant components, thus the scaling exponents are larger than 0.1 (Figure 3(a)). Whereas, when K is larger, for example 6 and 7, the scaling exponents do not always decrease with the IMF number increasing, and it is more obvious when $K = 7$ (Figure 3(c)), which indicates the IMFs are characterized by the low correlation. Figure 3(b) displays the scaling exponent

TABLE 1. Scaling exponents for different IMFs.

Number of IMFs	IMF1	IMF2	IMF3	IMF4	IMF5	IMF6	IMF7
3	0.6571	0.5861	0.2378	N/A	N/A	N/A	N/A
4	0.6571	0.5861	0.1995	0.1378	N/A	N/A	N/A
5	0.6571	0.5861	0.1752	0.1295	0.0439	N/A	N/A
6	0.6571	0.5861	0.1752	0.1295	0.2072	0.0176	N/A
7	0.6571	0.5861	0.1752	0.1503	0.0495	0.2072	0.0176

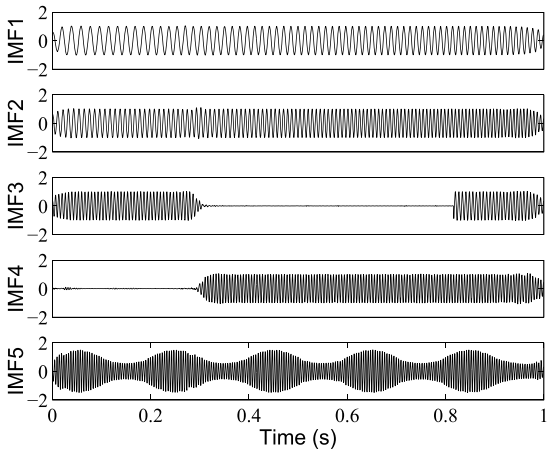

FIGURE 4. Decomposition of the simulated signal into its IMFs using FSSTH.

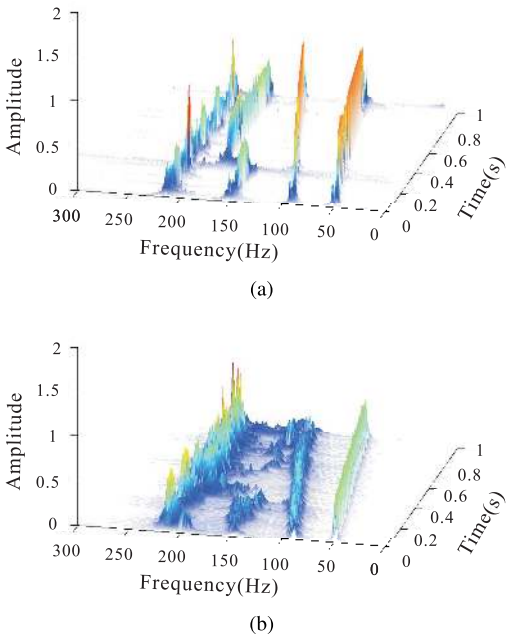

FIGURE 5. Time-frequency representation of the simulated signal by the proposed method (a) and the traditional SST (b), respectively.

when K is equal to 5, the IMF includes two kinds of components, and the α value of the last IMF is lower than 0.1. Based on the observations, we select 5 for K as an appropriate number of IMFs from FSSTH.

Figure 4 depicts the decomposed result of $s(t)$ by the FSSTH, five modes (IMF1-IMF5) are produced. It can be observed that the IMF1 and IMF2 are corresponding to low-frequency components that mainly result from $s_1(t)$ while the last three IMFs correspond to high-frequency components 150Hz, 180Hz, and 210Hz. Then, we calculate the instantaneous amplitudes and frequencies for each mode and generate the time-frequency representation (Figure 5(a)). As can be seen from Figure 5(a), the time-frequency map of the simulated signal is clearly shown, and the proposed method can effectively separate the two FM components in $s_1(t)$, the varying frequency at 0.3s in $s_2(t)$, and the AM component in $s_3(t)$. For comparison, the time-frequency representation of the same signal based on the traditional SST is shown in Figure 5(b), where one clearly sees the SST extracts two FM components in $s_1(t)$ and the AM component in $s_3(t)$, however, some interferences are emerging from 0.6s for $s_1(t)$. For $s_2(t)$, the mutation frequency cannot successfully identified, and some distortions are present simultaneously.

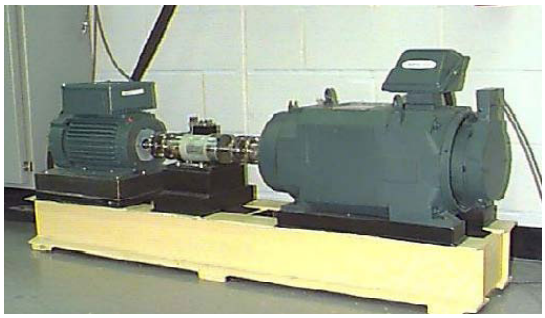

FIGURE 6. Experimental bearing test rig.

TABLE 2. Expected fault frequencies.

Fault category	Inner race	Outer race
Fault frequencies(Hz)	160.02	105.93

IV. EXPERIMENTAL EVALUATIONS

In this section, we apply the proposed method to the experimental signals in order to assess the validity of our approach further. We utilize the bearing dataset from Case Western Reserve University, which have been widely used to test new technologies. The rolling element test rig is shown in Figure 6, which is composed of 1.5kW induction motor, a torque transducer/encoder, a dynamometer, and control electronics [38]. The theoretical fault frequencies are reported in Table 2.

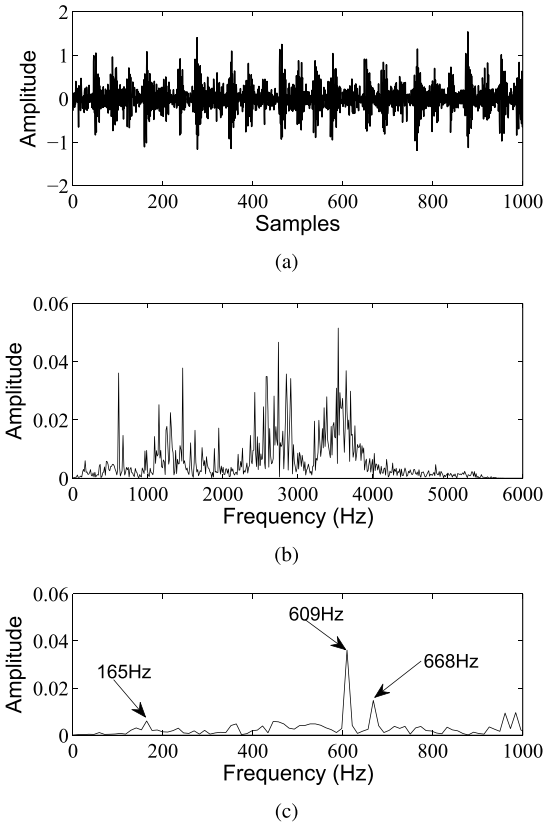

FIGURE 7. Time-domain waveform (a), Fourier spectrum (b) and local Fourier spectrum (c) of the vibration signal with inner race fault.

A. CASE FOR INNER RACE FAULT

The vibration signal and its spectrum from inner race fault dataset are plotted in Figure 7. It has been shown that many peaks appear in the Fourier spectrum (Figure 7(b)), however, it is difficult to directly detect the fault characteristic frequency (160.02Hz), even if the local Fourier spectrum is provided (Figure 7(c)), where the dominant frequencies are 609Hz and 668Hz. Thus, the proposed method is employed to analyze such vibration signal.

We perform the FSSTH into eight modes based on the scaling exponents obtained from DFA, which are shown in Figure 8. The IMF1 and IMF2 capture the lowest-frequency oscillations in the data, the IMF3, IMF4, IMF5 and IMF6 represent the middle-frequency components, and the rest of IMFs correspond to the highest-frequency contents in the vibration signal. Then, we calculate the instantaneous frequencies and amplitudes of the envelopes of the decomposed modes and obtain the time-frequency representation (Figure 9(a)). Meanwhile, we also provide a comparison with the traditional SST, and the corresponding result is illustrated in Figure 9(b). At first glance, it seems that both of the methods can successfully extract the fault feature frequency ($f_i = 160.02Hz$) and its harmonic ($2f_i$). However, if the close observation is kept, we will find that FSSTH does a better job capturing the characteristic frequencies with higher precision owing to obtaining more accurate instantaneous frequencies

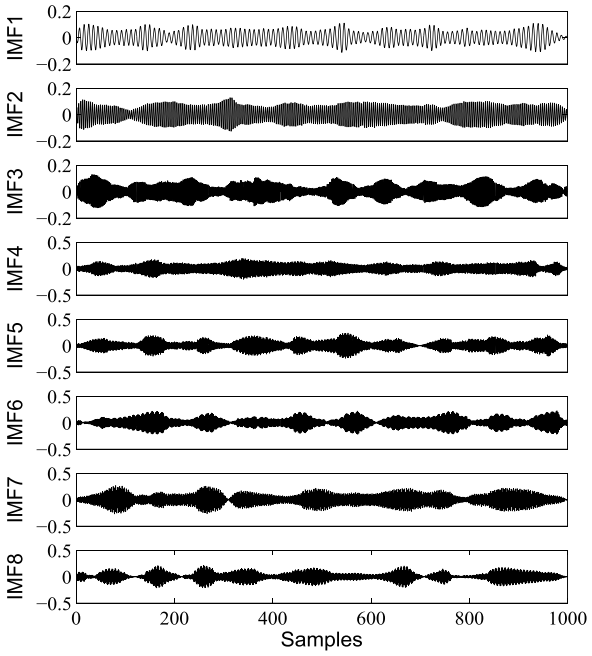

FIGURE 8. Decomposition of the vibration signal with inner race fault into its IMFs by FSSTH.

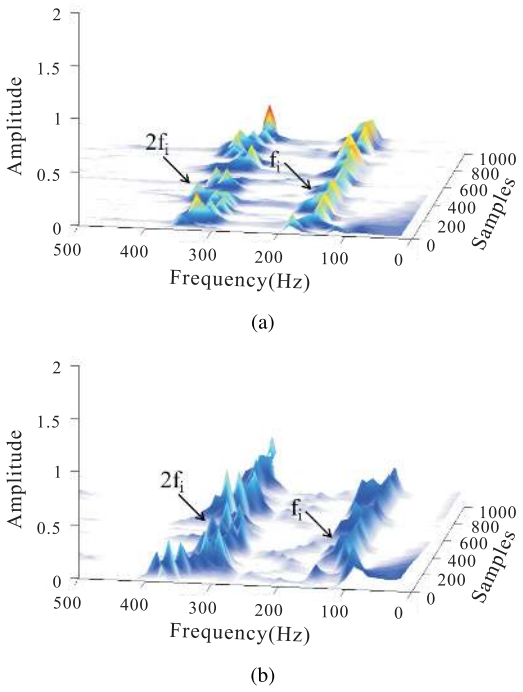

FIGURE 9. Time-frequency representation of the vibration signal with inner race fault by the proposed method (a) and the traditional SST (b), respectively.

using higher order approximations for the amplitude and phase compared with the traditional SST, which is beneficial with regard to confirmation of fault.

B. CASE FOR OUTER RACE FAULT

The vibration signal with the outer race fault and its spectrum are given in Figure 10. The spectrum (Figure 10(c))

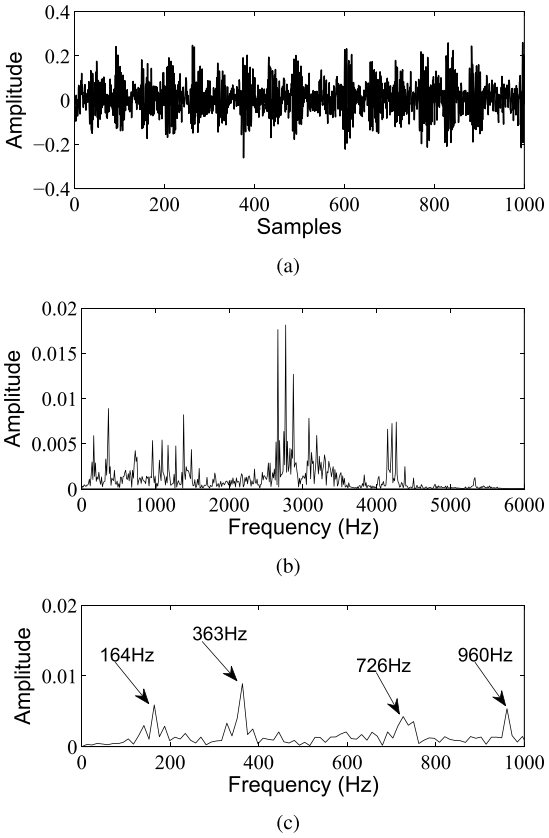

FIGURE 10. Time-domain waveform (a), Fourier spectrum (b) and local Fourier spectrum (c) of the vibration signal with outer race fault.

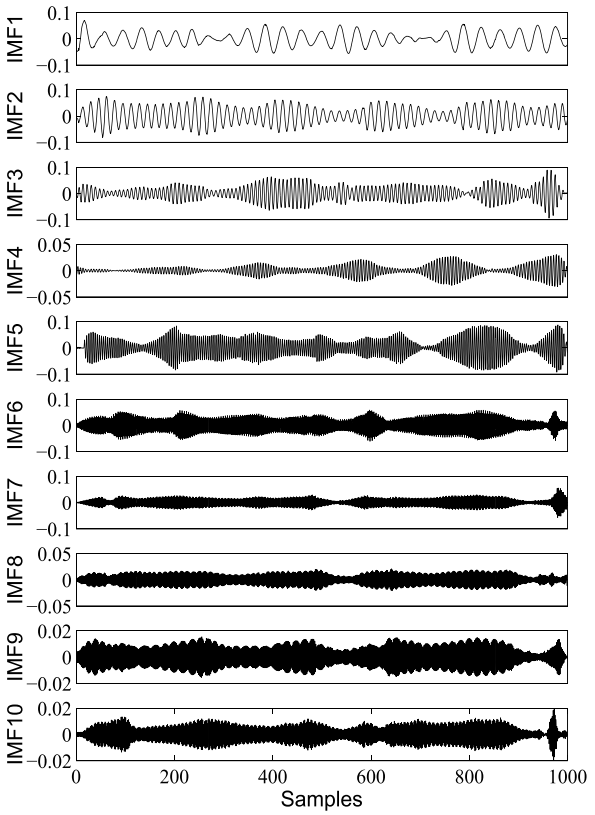

FIGURE 11. Decomposition of the vibration signal with outer race fault into its IMFs by FSSTH.

shows several dominant frequencies such as 164Hz, 363Hz, 726Hz and 960Hz. It is difficult to directly diagnose the fault frequency (105.93Hz) accurately from the spectrum.

Now, we apply the proposed approach to the vibration signal. Figure 11 describes the IMFs extracted by the FSSTH, where the number K is set to 10 according to the scaling exponents obtained from DFA. As reported in Figure 11, low order IMFs denote slow oscillations (IMF1-IMF4), and high order IMFs represent fast oscillations (IMF5-IMF10). Subsequently, the instantaneous frequencies and amplitudes of the envelopes are computed with respect to the decomposed modes, and the corresponding time-frequency representation is obtained, which is displayed in Figure 12(a). As a contrast, the time-frequency representation using the traditional SST is exhibited in Figure 12(b). Compared with the SST result, the proposed method performs clearly better. On the Figure 12, one notices that the fault characteristic frequency ($f_o = 105.93Hz$) associated with the outer race and the corresponding high harmonic frequencies ($2f_o$ and $3f_o$) are successfully extracted. Therefore, this gives us a clue that the outer race fault may occur in the rolling bearing. However, the traditional SST shows relatively the less information, only two frequency components, f_o and $2f_o$, appear, and some interferences are also present simultaneously in the vicinity of $2f_o$.

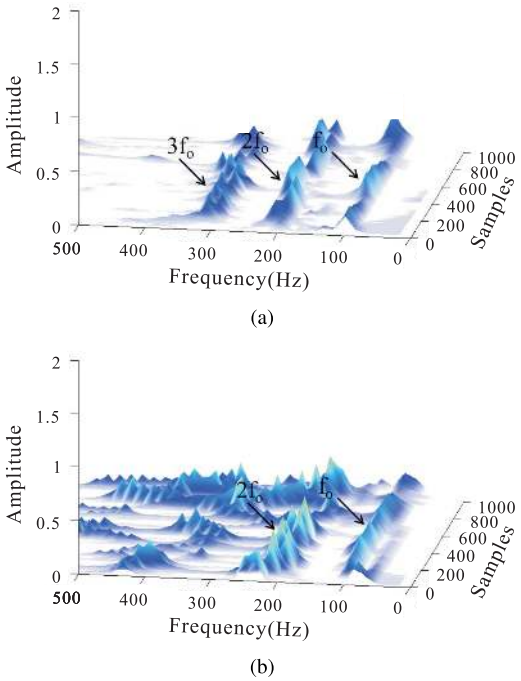

FIGURE 12. Time-frequency representation of the vibration signal with outer race fault by the proposed method (a) and the traditional SST (b), respectively.

V. CONCLUSION

Non-stationary signal analysis is an important issue for machine fault diagnosis, especially when the machine is

running under complex working conditions. In this paper, we have presented a new approach for rolling bearing fault diagnosis. First, the vibration signal is decomposed into a series of band-limited components by means of the high-order synchrosqueezing transform, and the detrended fluctuation analysis is used to determine the number of modes. Then, the time-frequency representation of the obtained modes or corresponding envelopes is exhibited in order to detect the fault feature frequencies associated with the rolling bearing. The effectiveness of the proposed method has been demonstrated by both simulation and experimental tests, which indicate that it is a promising tool for the fault diagnosis and condition monitoring of the rolling bearing. In our future work, the proposed method will be further investigated on the data from complex working conditions in mechanical equipment.

ACKNOWLEDGMENT

The authors would like to thank the editors and anonymous reviewers for their constructive comments which improved this paper greatly.

REFERENCES

[1] W. Wang, Q. Li, J. Gao, J. Yao, and P. Allaire, "An identification method for damping ratio in rotor systems," *Mech. Syst. Signal Process.*, vols. 68–69, pp. 536–554, Feb. 2016.
[2] X. Yu, F. Dong, E. Ding, S. Wu, and C. Fan, "Rolling bearing fault diagnosis using modified LFDA and EMD with sensitive feature selection," *IEEE Access*, vol. 6, pp. 3715–3730, 2018.
[3] B. Zhang, W. Li, X.-L. Li, and S.-K. Ng, "Intelligent fault diagnosis under varying working conditions based on domain adaptive convolutional neural networks," *IEEE Access*, vol. 6, pp. 66367–66384, 2018.
[4] Z. Jia, Z. Liu, C.-M. Vong, and M. Pecht, "A rotating machinery fault diagnosis method based on feature learning of thermal images," *IEEE Access*, vol. 7, pp. 12348–12359, 2019.
[5] W. Liu and W. Chen, "Recent advancements in empirical wavelet transform and its applications," *IEEE Access*, vol. 7, pp. 103770–103780, 2019.
[6] N. H. Chandra and A. Sekhar, "Fault detection in rotor bearing systems using time frequency techniques," *Mech. Syst. Signal Process.*, vols. 72–73, pp. 105–133, May 2016.
[7] I. Antoniadou, G. Manson, W. Staszewski, T. Barszcz, and K. Worden, "A time–frequency analysis approach for condition monitoring of a wind turbine gearbox under varying load conditions," *Mech. Syst. Signal Process.*, vols. 64–65, pp. 188–216, Dec. 2015.
[8] J. Allen, "Short term spectral analysis, synthesis, and modification by discrete Fourier transform," *IEEE Trans. Acoust., Speech, Signal Process.*, vol. ASSP-25, no. 3, pp. 235–238, Dec. 1977.
[9] H. Liu, L. Li, and J. Ma, "Rolling bearing fault diagnosis based on STFT-deep learning and sound signals," *Shock Vib.*, vol. 2016, Jul. 2016, Art. no. 6127479.
[10] Y. Chen, M. Bai, P. Anno, and Y. Chen, "Obtaining free USArray data by multi-dimensional seismic reconstruction," *Nature Commun.*, vol. 10, no. 1, pp. P4434–P4446, 2019.
[11] R. Yan, R. Gao, and X. Chen, "Wavelets for fault diagnosis of rotary machines: A review with application," *Signal Process.*, vol. 96, pp. 1–15, Mar. 2014.
[12] W. Liu, S. Cao, Z. Wang, K. Jiang, Q. Zhang, and Y. Chen, "A novel approach for seismic time-frequency analysis based on high-order synchrosqueezing transform," *IEEE Geosci. Remote Sens. Lett.*, vol. 15, no. 8, pp. 1159–1163, Aug. 2018.
[13] F. Auger and P. Flandrin, "Improving the readability of time-frequency and time-scale representations by the reassignment method," *IEEE Trans. Signal Process.*, vol. 43, no. 5, pp. 1068–1089, May 1995.
[14] Z. Feng, M. Liang, and F. Chu, "Recent advances in time–frequency analysis methods for machinery fault diagnosis: A review with application examples," *Mech. Syst. Signal Process.*, vol. 38, no. 1, pp. 165–205, Jul. 2013.
[15] R. Stockwell, L. Mansinha, and R. Lowe, "Localization of the complex spectrum: The S transform," *IEEE Trans. Signal Process.*, vol. 44, no. 4, pp. 998–1001, Apr. 1996.
[16] R. Wang, Y. Zhan, and H. Zhou, "Application of transform in fault diagnosis of power electronics circuits," *Scientia Iranica*, vol. 19, no. 3, pp. 721–726, Jun. 2012.
[17] J. O'Neill, P. Flandrin, and W. Williams, "On the existence of discrete Wigner distributions," *IEEE Signal Process. Lett.*, vol. 6, no. 12, pp. 304–306, Dec. 1999.
[18] M. Blodt, D. Bonacci, J. Regnier, M. Chabert, and J. Faucher, "On-line monitoring of mechanical faults in variable-speed induction motor drives using the Wigner distribution," *IEEE Trans. Ind. Electron.*, vol. 55, no. 2, pp. 522–533, Jan. 2008.
[19] S. G. Mallat and Z. Zhang, "Matching pursuit with time-frequency dictionaries," *IEEE Trans. Signal Process.*, vol. 41, no. 12, pp. 3397–3415, Dec. 1993.
[20] Z. Feng, J. Zhang, R. Hao, M. Zuo, and F. Chu, "Fault diagnosis of gearbox based on matching pursuit," in *Proc. Int. Conf. Wavelet Anal. Pattern Recognit.*, 2010, pp. 405–408.
[21] N. Huang, Z. Shen, S. Long, M. Wu, H. Shih, Q. Zheng, N. Yen, C. Tung, and H. Liu, "The empirical mode decomposition and the Hilbert spectrum for nonlinear and non-stationary time series analysis," *Proc. Roy. Soc. London A, Math., Phys. Eng. Sci.*, vol. 454, pp. 903–995, Mar. 1998.
[22] Y. Chen and J. Ma, "Random noise attenuation by *fx* empirical-mode decomposition predictive filtering," *Geophysics*, vol. 79, no. 3, pp. V81–V91, 2014.
[23] Z. Wu and N. E. Huang, "Ensemble empirical mode decomposition: A noise-assisted data analysis method," *Adv. Adapt. Data Anal.*, vol. 1, no. 1, pp. 1–41, Jan. 2009.
[24] Y. Lei, Z. He, and Y. Zi, "Application of the EEMD method to rotor fault diagnosis of rotating machinery," *Mech. Syst. Signal Process.*, vol. 23, no. 4, pp. 1327–1338, May 2009.
[25] M. Torres, M. Colominas, G. Schlotthauer, and P. Flandrin, "A complete ensemble empirical mode decomposition with adaptive noise," in *Proc. IEEE Int. Conf. Acoust., Speech Signal Process.*, May 2011, pp. 4144–4147.
[26] Y. Chen, G. Zhang, S. Gan, and C. Zhang, "Enhancing seismic reflections using empirical mode decomposition in the flattened domain," *J. Appl. Geophys.*, vol. 119, pp. 99–105, Aug. 2015.
[27] I. Daubechies, J. Lu, and H.-T. Wu, "Synchrosqueezed wavelet transforms: An empirical mode decomposition-like tool," *Appl. Comput. Harmon. Anal.*, vol. 30, no. 2, pp. 243–261, Mar. 2011.
[28] I. Daubechies and S. Maes, "A nonlinear squeezing of the continuous wavelet transform based on auditory nerve models," in *Wavelets in Medicine and Biology*, A. Aldroubi and M. Unser, Eds. Boca Raton, FL, USA: CRC Press, 1996, pp. 527–546.
[29] C. Li and M. Liang, "Time–frequency signal analysis for gearbox fault diagnosis using a generalized synchrosqueezing transform," *Mech. Syst. Signal Process.*, vol. 26, pp. 205–217, Jan. 2012.
[30] G. Thakur and H.-T. Wu, "Synchrosqueezing-based recovery of instantaneous frequency from nonuniform samples," *SIAM J. Math. Anal.*, vol. 43, no. 5, pp. 2078–2095, Jan. 2011.
[31] D. Pham and S. Meignen, "High-order synchrosqueezing transform for multicomponent signals analysis—With an application to gravitational-wave signal," *IEEE Trans. Signal Process.*, vol. 65, no. 12, pp. 3168–3178, Mar. 2017.
[32] Y. Hu, X. Tu, F. Li, and G. Meng, "Joint high-order synchrosqueezing transform and multi-taper empirical wavelet transform for fault diagnosis of wind turbine planetary gearbox under nonstationary conditions," *Sensors*, vol. 18, no. 2, pp. 150–167, Jan. 2018.
[33] X. Tu, Y. Hu, F. Li, S. Abbas, Z. Liu, and W. Bao, "Demodulated high-order synchrosqueezing transform with application to machine fault diagnosis," *IEEE Trans. Ind. Electron.*, vol. 66, no. 4, pp. 3071–3081, Apr. 2019.
[34] C.-K. Peng, S. V. Buldyrev, S. Havlin, M. Simons, H. E. Stanley, and A. L. Goldberger, "Mosaic organization of DNA nucleotides," *Phys. Rev. E, Stat. Phys. Plasmas Fluids Relat. Interdiscip. Top.*, vol. 49, no. 2, pp. 1685–1689, Jul. 2002.
[35] A. Mert and A. Akan, "Detrended fluctuation thresholding for empirical mode decomposition based denoising," *Digit. Signal Process.*, vol. 32, pp. 48–56, Sep. 2014.
[36] F. Li, B. Zhang, S. Verma, and K. J. Marfurt, "Seismic signal denoising using thresholded variational mode decomposition," *Explor. Geophys.*, vol. 49, no. 4, pp. 450–461, Aug. 2018.

[37] Y. Liu, G. Yang, M. Li, and H. Yin, "Variational mode decomposition denoising combined the detrended fluctuation analysis," *Signal Process.*, vol. 125, pp. 349–364, Aug. 2016.
[38] B. Merainani, C. Rahmoune, D. Benazzouz, and B. Ould-Bouamama, "Rolling bearing fault diagnosis based empirical wavelet transform using vibration signal," in *Proc. 8th Int. Conf. Modelling, Identificat. Control*, 2016, pp. 526–531.

WEI LIU received the B.E. degree in exploration geophysics from the China University of Petroleum (East China), Qingdao, China, in 2006, and the M.S. degree in exploration geophysics and the Ph.D. degree in geological resources and geological engineering from the China University of Petroleum (Beijing), Beijing, China, in 2009 and 2016, respectively. He is currently working as a Lecturer with the Beijing University of Chemical Technology. His research interests include signal analysis and processing, seismic data processing and interpretation, and mechanical fault diagnosis.

WEI CHEN received the B.E. and Ph.D. degrees in geophysics from the China University of Petroleum (Beijing), in 2008 and 2016, respectively. He is currently an Associate Professor with Yangtze University. His research interests include seismic signal analysis, time-frequency analysis, and seismic data processing.

ZHIHUA ZHANG received the B.E. degree in safety science and engineering from the North University of China, in 2018. He is currently pursuing the M.E. degree with the Beijing University of Chemical Technology. His research interests include signal analysis, deep learning, and intelligent fault diagnosis.